

Identification of inhibitors of the RGS homology domain of GRK2 by docking-based virtual screening

Emiliana Echeverría, Ana Julia Velez Rueda, Maia Cabrera, Ezequiel Juritz, Valeria Burghi, Lucas Fabián, Carlos Davio, Pablo Lorenzano Menna, Natalia Cristina Fernández



PII: S0024-3205(19)30799-4
DOI: <https://doi.org/10.1016/j.lfs.2019.116872>
Reference: LFS 116872

To appear in: *Life Sciences*

Received date: 10 May 2019
Revised date: 10 September 2019
Accepted date: 11 September 2019

Please cite this article as: E. Echeverría, A.J.V. Rueda, M. Cabrera, et al., Identification of inhibitors of the RGS homology domain of GRK2 by docking-based virtual screening, *Life Sciences*(2019), <https://doi.org/10.1016/j.lfs.2019.116872>

This is a PDF file of an article that has undergone enhancements after acceptance, such as the addition of a cover page and metadata, and formatting for readability, but it is not yet the definitive version of record. This version will undergo additional copyediting, typesetting and review before it is published in its final form, but we are providing this version to give early visibility of the article. Please note that, during the production process, errors may be discovered which could affect the content, and all legal disclaimers that apply to the journal pertain.

Identification of inhibitors of the RGS homology domain of GRK2 by docking-based virtual screening

**Emiliana Echeverría¹, Ana Julia Velez Rueda², Maia Cabrera³,
Ezequiel Juritz⁴, Valeria Burghi¹, Lucas Fabián⁵, Carlos Davio¹,
Pablo Lorenzano Menna^{3,6}, Natalia Cristina Fernández¹**

1. Instituto de Investigaciones Farmacológicas (ININFA-UBA-CONICET), Facultad de Farmacia y Bioquímica, Universidad de Buenos Aires, Buenos Aires, Argentina.
2. Structural Bioinformatics Group, Department of Science and Technology, National University of Quilmes - CONICET, Roque Sáenz Peña 352, (1876) Bernal, Provincia de Buenos Aires, Argentina.
3. Laboratorio de Farmacología Molecular, Departamento de Ciencia y Tecnología, Universidad Nacional de Quilmes- CONICET, Roque Sáenz Peña 352, Bernal, B1876BXD, Buenos Aires, Argentina.
4. Center for Bioinformatics and Integrative Biology, Facultad de Ciencias de la Vida, Universidad Andrés Bello, 8370146, Santiago, Chile.
5. Instituto de Química y Metabolismo del Fármaco (IQUIMEFA-UBA-CONICET), Facultad de Farmacia y Bioquímica, Universidad de Buenos Aires, Buenos Aires, Argentina.
6. Max Planck Laboratory for Structural Biology, Chemistry and Molecular Biophysics of Rosario (MPLbioR, UNR-MPIbpC) and Instituto de Investigaciones para el Descubrimiento de Fármacos de Rosario (IIDEFAR, UNR-CONICET), Universidad Nacional de Rosario, Ocampo y Esmeralda, S2002LRK Rosario, Argentina.

Abstract

Aims

G protein-coupled receptor (GPCR) kinases (GRKs) are mainly involved in the desensitization of GPCRs. Among them, GRK2 has been described to be upregulated in many pathological conditions and its crucial role in cardiac hypertrophy, hypertension, and heart failure promoted the search for pharmacological inhibitors of its activity. There have been several reports of potent and selective inhibitors of GRK2, most of them directed to the kinase domain of the protein. However, the homologous to the regulator of G protein signaling (RH) domain of GRK2 has also been shown to regulate GPCRs signaling. Herein, we searched for potential inhibitors of receptor desensitization mediated by RH domain of GRK2.

Materials and methods

We performed a docking-based virtual screening utilizing the crystal structure of GRK2 to search for potential inhibitors of the interaction between GRK2 and Gαq protein. To evaluate the biological activity of compounds we measured, calcium response of histamine H1 receptor (H1R) using Fura-2AM dye and H1R internalization by saturation binding experiments in A549 cells. GRK2(45-178)GFP translocation was determined in HeLa cells through confocal fluorescence imaging.

Key findings

We identified inhibitors of GRK2 able to reduce the RH mediated desensitization of the histamine H1 receptor and GRK2 translocation to plasma membrane. Also candidates presented adequate lipophilia and cytotoxicity profile.

Significance

We obtained compounds with the ability of reducing RH mediated actions of GRK2 that can be useful as a starting point in the development of novel drug candidates aimed to treat pathologies where GRK2 plays a key role.

Keywords

GRK2, GPCR, DBVS, CADD, RH, PPI

1. Introduction

G protein-coupled receptor (GPCR) kinases (GRKs) are key regulators of the largest family of membrane receptors involved in signal transduction. GPCRs modulate a multitude of physiological processes, and their dysregulation contributes to many diseases, being the targets of ~35% of Food and Drug Administration approved drugs [1].

In mammals there have been identified seven members belonging to GRK family of proteins which have been classified into three subfamilies according to their amino acids sequence and tertiary structure homology: visual GRKs (GRK1, and GRK7), GRK2 subfamily (GRK2 and GRK3), and GRK4 subfamily (GRK4, GRK5 and GRK6). Whereas GRK1 and 7 are specifically expressed in retinal cells and GRK4 in testis, the rest of GRKs (GRK2, 3, 5, and 6) are ubiquitously expressed [2–4]. The protein structure of GRKs consists of three structural and functional well defined domains: an N-terminal domain homologous to the regulator of G protein signaling (RH domain) that is involved in receptor recognition, a central highly conserved catalytic domain with kinase activity, and a C-terminal domain responsible of subcellular localization and agonist dependent translocation to plasma membrane [5].

In particular, GRK2 was originally described to specifically phosphorylate the C-terminal tails or cytoplasmic loops of active GPCRs, promoting binding of β -arrestin proteins to the receptor hence inhibiting interactions with heterotrimeric G proteins and further signaling [6]. This process known as homologous desensitization, is an adaptive mechanism aimed to prevent receptor overstimulation. There are several relevant pathological situations where GPCRs signaling is dysregulated by a variety of mechanisms related to GRK2 multifunctional role, indicating the physiological importance of this protein in disease progression. GRK2 levels and activity have been reported to be increased in patients or in preclinical models of cardiac hypertrophy, hypertension, heart failure, obesity and insulin resistance conditions. Accordingly, pharmacological inhibition of GRK2 or genetic deletion proved to be cardioprotective in cardiovascular and metabolic diseases [7]. On the other hand, alterations in GRK2 levels in immune cells have been described to play an important role in the development of inflammation and have been associated to Alzheimer, multiple sclerosis and rheumatoid arthritis where GRK2 was proposed as a viable therapeutic target [8–11]. In the last decades a growing body of evidence showed that GRK2 may also regulate downstream activity of GPCRs independently of receptor phosphorylation. Desensitization of GPCRs signaling independently of kinase activity has been described for adenosine type 1 receptor (A1R) and μ -opioid receptor (μ OR) [12], metabotropic glutamate receptor 5 (mGluR5) [13], histamine H1 and H2 receptors (H1R and H2R) [14,15], lysophosphatidic acid (LPA1) receptor [16], endothelin receptor type B (ETb) [8], follicle-stimulating hormone receptor [17] and D2 dopamine receptor [18] among others. Even more, direct interaction of GRKs with signaling molecules downstream of GPCRs has been described [19] and in

some cases expression of the RH domain of GRK2 resulted sufficient for attenuating receptor signaling through Gαq activation [20,21].

Although targeting GRK2 emerges as a potentially relevant approach to treat pathological conditions [22,23] the search of selective and potent GRK2 inhibitors has presented many difficulties, mainly due to the lack of specific blockage of GRK2. While inhibition of the pleckstrin homology domain of GRK2 proved to be a successful strategy, most kinase inhibitors acting as ATP-competitive inhibitors displayed some degree of activity towards other GRKs or even other members of the AGC family of kinases as PKA or ROCK [24].

In this work we performed a docking-based virtual screening (DBVS) directed to the RH domain of GRK2. We identified candidates that inhibited RH mediated desensitization of GPCRs and GRK2 translocation to plasma membrane. Through this strategy we achieved novel drug candidates with the ability of interfering with phosphorylation independent actions of GRK2 that may be useful for treatment of conditions where GRK2 plays a crucial role.

2. Materials and Methods

2.1. Chemicals and plasmid constructions

Bovine serum albumin (BSA), fura-2 acetoxymethyl ester (Fura-2AM), histamine dihydrochloride, mepyramine, triton X-100 and pluronic acid, were obtained from Sigma Chemical Company (St. Louis, MO, United States). CMPD101 was acquired from Tocris Cookson Inc. (Ballwin, MO). [³H]mepyramine was purchased from Perkin Elmer Life Sciences (Boston, MA). Screening compounds were acquired from Enamine Ltd. (Monmouth, NJ). Fetal calf serum was from Natocor (Argentina). Other chemicals used were of analytical grade and obtained from standard sources.

pcDNA3-GαqQL was a generous gift from Dr O. Cosso (IFIBYNE, UBA-CONICET, Argentina). pcDNA3-GRK2D110A and pcDNA3-GRK2K220R was kindly provided by Dr. J. Benovic (Thomas Jefferson University, Department of Microbiology and Immunology, Kimmel Cancer Center, Philadelphia, USA). pEGFP-HAGRK2(45-178)GFP was a generous gift from Dr. P. Wedegaertner, (Thomas Jefferson University, Philadelphia, PA, USA).

The following primary antibodies were purchased from Santa Cruz Biotechnology, CA:

Anti-β-tubulin (IgG from rabbit / catalogue#SC-9104 / Lot#F1210 / final dilution: 1/500)

Anti-GRK2 (IgG from rabbit / catalogue#SC-562 / Lot#F1610 / final dilution: 1/1000)

The secondary antibody Anti-rabbit (IgG from goat / catalogue#PI1000 / Lot#X0126 / final dilution: 1/4000) was purchased from Vector Laboratories, CA.

2.2. Conformational analysis

The human GRK2 crystal structures were retrieved from the Protein Data Bank (PDB). A total number of seven conformations, excluding mutants, were used for the analysis.

The z-scores derived from C-alpha RMSD per position of the maximum-pair of conformers were calculated using ProFit software and the results were expressed as [25]:

$$\text{z-score} = \text{RMSD position} - \text{RMSD average} / \text{standard deviation}$$

The number of cavities and tunnels, as well as their properties, were estimated for all conformers using Fpocket [26]. The solvent accessibility per residue was calculated using NACCES software [27].

All data obtained were retrieved and processed using our own scripts coded in Python.

2.3. Virtual screening and data visualization

In order to identify potential inhibitors of RH domain of GRK2, we performed a docking based virtual screening (DBVS) using an opened conformation of GRK2 (PDB ID:3KRW_A), with the biologically relevant residues Arg106 and Gln133 exposed to the solvent. The database employed in the DBVS was the publicly available Enamine Advanced Collection (available online: <https://www.enamine.net>). In this study, the pocket containing the residues Arg106 and Gln133 of the RH domain of human GRK2 was used as a target. The docking was centered in the alpha carbon of Leu136, with a grid size of 22 Å. AutoDock Vina [28] was used as DBVS software. The docking assay for the top hundred compounds was repeated one hundred times to confirm the massive screening results. Results obtained with AutoDock Vina were also confirmed with Autodock 4.2 [29]. The chemical compounds displaying the highest docking scores in the calculations were used for the *in vitro* activity assays.

2.4. Cell culture and transfection

A549 (human lung carcinoma epithelial cells, ATCC # CCL-185), HepG2 (human hepatocellular carcinoma epithelial cells ATCC # HB-8065) and HeLa (human cervix adenocarcinoma epithelial cells, ATCC # CCL-2) cells were cultured in Dulbecco's Modified Eagle's Medium (DMEM) and U937 (human histiocytic lymphoma promonocytic cells ATCC # CRL-1593.2) in RPMI 1640 medium, all supplemented

with 10% fetal calf serum and 50mg/ml gentamicin. Cultures were maintained at 37°C in humidified atmosphere containing 5% CO₂.

For transient transfections, A549 or HeLa cells were grown to 80–90% confluency and the cDNA constructs were transfected using the K2 Transfection System (Biontex, Munich, Germany). The transfection protocol was optimized as recommended by the suppliers. Assays were performed 48 h after transfection.

2.5. Western Blot assays

For western blot assays, cells were lysed in 50mM Tris–HCl pH 6.8, 2% SDS, 100mM 2-mercaptoethanol, 10% glycerol and 0.05% bromophenol blue and sonicated to shear DNA. Total cell lysates were resolved by SDS-PAGE. Blots were incubated with anti-beta tubulin and anti-GRK2 primary antibodies (Santa Cruz Biotechnology, CA), followed by horseradish peroxidase conjugated anti-rabbit antibody (Vector Laboratories, CA; see materials for details) and developed by enhanced chemiluminescence (ECL) following the manufacturer's instructions (Amersham Life Science, England).

2.6. Intracellular calcium measurements

Changes in intracellular Ca²⁺ concentration were measured using Fura-2AM fluorescent indicator. A549 cells were seeded in 96 wells dishes for 24h (90–100% confluence). Thereafter, culture media was replaced by loading buffer (140mM NaCl, 3.9mM KCl, 0.7mM KH₂PO₄, 0.5mM Na₂HPO₄, 1mM CaCl₂, 0.5mM MgCl₂, 10mM glucose, 0.1% BSA, 20mM HEPES, pH 7.4) containing 4mM Fura-2AM and 0.2% pluronic acid and cells were incubated for 90 min at 37°C in humidified atmosphere containing 5% CO₂ to facilitate the hydrolysis of the ester to the acid form. Excess

dye was removed by washing cells with loading buffer. Fluorescence was measured in a FlexStation 3 microplate reader (Molecular Devices Inc., San Jose, CA, United States). The wavelength was set at 340 and 380 nm, and detection was at 500 nm. After 30 s of initial recording to determine basal levels, 100 μ M Histamine and the time course of intracellular Ca^{2+} mobilization was recorded for 180 s. At the end of the time course, Triton X-100 (0.25% v/v) was added to determine F_{max} . Basal levels (B) were determined as the media of the recorded measurements in the first 30 s for each well. Autofluorescence was quantified by measuring the fluorescence produced by an equivalent suspension of not-loaded cells. Results were expressed as the ratio of fluorescence's 340/380 (X) normalized according to: $X'=(X-B)/(F_{max}-B)$. For desensitization experiments, A549 cells were treated with 10, 33 or 100 μ M or vehicle histamine in the last 10 min of incubation with the Fura-2AM dye. Thereafter, cells were washed twice with loading buffer and assay proceeded in the same way as indicated before.

For biological activity screening of Enamine compounds, A549 cells loaded with Fura-2AM were pretreated with 100nM of C1-C15 or DMSO during 40 min, and response and desensitization experiments were performed.

2.7. Internalization assay

A549 cells were incubated (internalized) or not (control) for 60 min with 100 μ M histamine and after washing, the number of receptor sites was analyzed by radioligand-binding assay. CMPD101 10 μ M or C13Z34 100nM inhibitors were added 20 min prior to histamine treatment and their concentrations were maintain during incubation with histamine. For binding studies, duplicate saturation assays were performed by incubating 1×10^5 A549 cells in 50mM Tris-HCl, pH 7.4, for 90 min at

4°C with increasing concentrations of [³H]mepyramine in the absence or presence of 10µM unlabeled mepyramine. Specific binding was calculated by subtraction of nonspecific binding from total binding. The incubation was stopped by washing two times with ice-cold saline solution. Experiments on intact cells were carried out at 4°C to avoid ligand internalization.

2.8. GRK2 translocation assays

HeLa cells were seeded in 35mm plates and transfected with pEGFP-HAGRK2(45-178)GFP alone or in combination with pcDNA3-GαqQL. After 24 h, cells were seeded in polylysinated glass at 15% confluence and 24 h later cells were starved for 4 h and then treated with the indicated compounds at 100nM for 30 min. Cells were then washed with PBS, fixed in 4% formaldehyde in PBS for 15 min and washed again. Images were examined using an Axio Observer.Z1 microscope (Carl Zeiss Microscopy GmbH, Germany; Objective LCI Plan-Neofluar 63x/1,30 Imm Korr DIC M27; Optovar 1x Tubelens; ZEISS Filter set 38 HE - eGFP, BP 470/40, FT 495, BP 525/50, and AxioCam HRm3 S/N 631 camera (adaptor 0,63x; exposition time 500-900ms; focus 0,86µm). Intensity profiles were performed using Image J software.

2.9. Cytotoxicity determination assays

HepG2 and U937 cells were treated with increasing concentrations, ranging from 333nM to 100µM, of C5Z29, C9Z81, C13Z34 or DMSO during 48hs. Cell viability was determined by Trypan Blue exclusion and counting in Neubauer chamber.

2.10. Determination of the experimental lipophilicity

Experimental logarithms of capacity factor ($\log k$) were calculated by liquid chromatography (HPLC, Waters 590 HPLC Pump) with an ultraviolet detector (320–336 nm, Jasco-975, Software WinPcChrom XY, Jasco Inc, Easton, MD, USA) and a Sunfire column C18, 5.0 mm, 4.6 x 150 mm (Waters Corp., Milford, MA, USA). Stock solutions of each TSC in DMSO (3.5 mg/ml) were injected (10 μ l) and a mobile phase composed of acetonitrile–buffer phosphate pH 7.0 (29 mM) of different volume ratios (20 : 80, 25 : 75, 30 : 70, 40 : 60, 45 : 55, 50 : 50 and 55 : 45) was pumped at a flow rate of 1.0 ml/min. Logarithms of capacity factor ($\log k$) were calculated as follows:

$$\log k = \log[(t_r - t_0)/t_0]$$

Being t_r and t_0 the retention time and the dead time (solvent front, DMSO) respectively. A curve of $\log k$ versus the percentage of acetonitrile (%) in the mobile phase was built and $\log k_{\text{water}}$ ($\log k_w$) values were extrapolated at 0% acetonitrile [30].

2.11. Statistical Analysis

Numbers (n) for all experiment are provided in corresponding figures and refer to independent measurements. Fittings of sigmoidal concentration-response and comparison of best fit values according to extra-sum of squares F test were performed with GraphPad Prism 5.00 for Windows, GraphPad Software (San Diego, CA).

Statistics were performed using GraphPadInStat version 3.01, GraphPad Software (San Diego, CA). Comparisons were made using Two-way ANOVA followed by the Tukey's post-test, with Post-hoc test being run only if F achieved $P < 0.05$ and there

was no significant variance in homogeneity. Different letters indicate statistically significant differences. The level of significance was set at $P < 0.05$.

3. Results

3.1. *In Silico* conformational diversity analysis of GRK2 crystallographic structures and target selection

It has been described that action of RH domain of GRK2 depends on the PPI surface between GRK2 and the Gαq protein [31]. Based on that, structural analysis of biologically relevant pockets and their accessibility was carried out [32] as well as the identification of those relative small regions or hot spots, that govern the PPI surface since are responsible for the disproportionate contribution to the binding energy between the two proteins [33].

It is well established that the crystal structures of the same protein from different crystallization conditions, are informative about the structural dynamics of the protein [34]. Also, it is well known that different protein conformations may differ in the number and physicochemical properties of their tunnels and cavities, which is also related with the protein functionality [32, 35]. Thus, protein flexibility is a fundamental requirement for most biological functions, and indeed, protein functionality is poorly understood if only a single structure is considered [36]. In order to take into account the protein conformational diversity for the analysis, all the crystal structures of GRK2 available in the Protein Data Bank (PDB) were retrieved [37]. After excluding those with mutations, a total number of 7 conformers were obtained for the structural analysis based on the characteristics of biologically relevant pockets. The number of pockets were similar in all conformations, nevertheless some conformations presented the residues Arg106 and Gln133 exposed, with the accessible surface

area for these residues 68.0% and 130.7% bigger than the mean values for these positions within the conformers (75.0 \AA^2 and 54.6 \AA^2 respectively, with a mean value for all the residues of 32.51 \AA^2). Such residues were identified as necessary for GRK2 binding with Gαq through a mutational analysis [38]. We also calculated the Z-Scores derived from C-alpha RMSD per position of the maximum-pair of conformers, focusing on the residues involved in the RH-Gαq PPI as described in Materials and Methods. The Z-Score distribution revealed that residues Arg106 and Gln133, are located in a relatively low mobility region within human GRK2 structure, contributing to the idea that this zone is an appropriate target for small molecules in order to interfere RH-Gαq interaction (Fig. 1a).

To predict the hot spots that could govern the PPI between GRK2 and Gαq (Fig 1b) we used the knowledge-based fade and contacts (KFC) server, which is based upon the three-dimensional structure of a PPI complex [39], in this case the one between bovine GRK2 and chimera Gαq available in the PDB ID: 2BCJ [41]. According to KFC predictions, residues Arg106, Phe109, Asp110, Met114, Lys115, Leu118, Ala119, and Gln133 on GRK2 are those who contributes the most to interaction with Gαq (Fig 1c, purple font). Some of them proved to be fundamental in the interaction between GRK2 and Gαq in experimental assays [40] (Fig 1c, boxed residues). These results were considered when defining the specific molecular target for inhibitors search on human GRK2 of PDB ID: 3KRW [41] (Fig 1d).

3.2. Virtual Screening

In order to identify novel PPI inhibitors of the GRK2RH/Gαq interface, we performed a DBVS using the library “Advanced Collection from Enamine”, which contains more than 400,000 drug-like compounds characterized by $MW \leq 350$, $cLogP \leq 3$, and

rotatable bonds \leq 7 (<https://www.enamine.net>). An opened conformation (PDB ID: 3KRW), with exposed biological relevant residues, was taken as reference for the virtual screening analysis. The grid box was built considering the cavities' volume and drug score information. Cavities which maximized those parameters and contained biologically relevant residues were included. As result of DBVS using AutoDock Vina [28], a ranking of candidate compounds was obtained. These compounds were ordered by docking energy, being preferred those candidates with lower values. After visual inspection of the poses of the compounds displaying the bests docking scores, we chose 15 of them which were acquired from Enamine (Fig. 2).

3.3. *In Vitro* Screening of the Candidate Compounds

With the aim of determining if the candidate compounds show the desired inhibitory effect, we measured whether these molecules were able to inhibit GRK2 mediated receptor desensitization. We used as biological model A549 cell line, that endogenously expresses GRK2 and histamine H1 receptor (H1R), a G α_q coupled receptor that proved to be desensitized by the RH domain of GRK2 [14]. Intracellular calcium levels were determined using Fura-2AM dye in naïve cells stimulated with the agonist histamine ("response assays") and in desensitized cells stimulated with histamine ("desensitization assays"). For evaluation of receptor response, Fura-2AM loaded A549 cells were stimulated with 1 μ M, 10 μ M and 100 μ M histamine (HA). A concentration dependent calcium response was observed (Fig. 3a, left panel). For evaluation of receptor desensitization A549 cells were pre-exposed to 10 μ M and 100 μ M HA during 10 min, washed and stimulated with 100 μ M HA to determine the capacity of the system to evoke a new calcium response. Pretreatment of cells with

agonist lead to a concentration dependent reduction in calcium response to HA (Fig. 3a, right panel). Based on these results, stimulus with 100 μ M HA and pretreatment with HA 100 μ M was chosen for evaluation of compounds in response and desensitization experiments respectively. To verify if our system was able to evidence an alteration in the function of RH domain of GRK2, we transfected A549 cell line with a dominant negative mutant of GRK2 that is unable to bind G α q (GRK2-D110A). Mutant overexpression (Fig. 3b, right panel) potentiated calcium response to HA and almost dampened H1R desensitization increasing calcium response even in cells pre-exposed to HA (Fig. 3b, left panel).

To identify RH inhibitors, A549 cells were incubated during 40 min with candidate compounds at 100nM and response and desensitization assays were performed. Among the 15 molecules evaluated, 3 of them: C5Z29, C9Z81 and C13Z34, significantly increased calcium response to HA in both naïve and desensitized cells as compared to vehicle control, where compound C13Z34 led to the greater increments on calcium response (Fig.4a). To verify whether these compounds act by inhibiting GRK2 RH domain we overexpressed GRK2-D110A which is unable to interact with G α q protein and in consequence should be insensitive to the action of compounds only if they act by blocking GRK2 RH interaction with G α q protein. None of the active compounds modified H1R stimulated calcium response in cells transfected with GRK2-D110A (Fig. 4b). Moreover, none of the active compounds have activity *per se* over intracellular calcium basal levels at the concentrations assayed (Fig. 4c), indicating that the observed effects over calcium levels depends on receptor activation regulation mediated by the RH domain of GRK2.

Since C13Z34 induced a reversion in H1R desensitization, almost restoring calcium response to that of untreated cells, concentration-response curves for

desensitization experiments were performed. Pretreatment with C13Z34 concentration-dependently increased calcium response in desensitized cells with a pIC_{50} for GRK2 inhibition of 9.13 ± 0.48 (Fig. 5a). Interestingly, in presence of a dominant negative mutant of GRK2 lacking phosphorylation activity (GRK2-K220R), C13Z34 also increased H1R response by diminishing H1R desensitization indicating that its action is preserved even over GRK2 kinase death mutant (Fig. 5b). Consistently, pretreatment with CMPD101, a potent and selective inhibitor of GRK2 and GRK3 kinase activity did not modified H1R calcium response nor inhibited short term desensitization of the H1R (Fig. 5c). Since H1R internalization depends on GRK2 kinase activity we evaluated whether C13Z34 inhibited a phosphorylation dependent mechanism. After 1 h exposure of A549 cells to HA 100 μ M the number of H1R membrane sites diminished to the $65.8 \pm 2.2\%$ of control basal levels (Fig. 5d). CMPD101 completely abolished H1R internalization restoring membrane receptor number to that of untreated cells. Conversely, although C13Z34 significantly inhibited H1R internalization (80.5 ± 3.4 vs $65.8 \pm 2.2\%$ membrane sites; $P < 0.05$) it was not able to restore basal levels $P < 0.05$ (Fig. 5d).

When the interactions and spatial arrangement of active compounds in the druggable pocket was analyzed through the study of the obtained docking poses, we found in all cases, close contacts with the protein's residues, including Arg106 and Gln133. Consistently with previous results, only compound C13Z34 was able to establish H-bonds, being residue Gln133 involved in the interaction (Fig. 5e).

Correct function of GRK2 requires rapid spatial and temporal regulation. Since GRK2 is a cytosolic protein that migrates to plasma membrane to exert its desensitizing action [42] we evaluate whether our candidates were able to block GRK2 redistribution to areas of active signaling through confocal fluorescence imaging,

using HeLa cells transfected with GRK2(45-178)GFP, consisting in the RH domain of GRK2 fused to green fluorescent protein. The fluorescence intensity was quantified in each image using line intensity profiles across each one of the cells. The presence of peaks at the beginning and the end of the profile indicates increased concentration of GRK2(45-178)GFP at the cell margins (Fig. 6). As expected, GRK2(45-178)GFP showed cytoplasmic localization (Fig. 6a, left panel). However, after coexpression of the construct with a constitutively active variant of Gαq protein (GαqQL), GRK2 redistributed to plasma membrane (Fig. 6a, right panel). To verify compounds action, HeLa transfected cells were incubated during 30 min with 100nM C5Z29, C9Z81 or C13Z34, or vehicle (DMSO). GRK2 redistribution to plasma membrane when GαqQL is coexpressed was dampened by C5Z29, C9Z81 or C13Z34 pretreatment, but not by compound used as negative control or by the vehicle, DMSO (Fig 6b).

Finally, we determined relevant pharmacokinetics characteristics of compounds in order to obtain preliminary information useful for future optimization of candidates. Evaluation of cytotoxicity was carried out in HepG2 and promonocytic U937 cells as indicators of hepatic and systemic cytotoxicity. Cells were incubated during 48 h with compounds' concentrations ranging from 333nM to 100μM, and cellular viability was determined by trypan blue exclusion and counting in Neubauer chamber. Among compounds evaluated, only C9Z81 displayed cytotoxicity in both cell lines killing up to the 80% of HepG2 and U937 cells and showing an $CC_{50} > 500\mu M$ and of $16.8 \pm 1.25\mu M$ respectively (Fig. 7a). Since lipophilicity may impact in every ADMET properties of a molecule, and the $\log K_w$ reflects the $\log P$ of a molecule, we determined the experimental $\log K_w$ of compounds as a lipophilicity indicator, through High Performance Liquid Chromatography in Reverse Phase (RP-HPLC), obtaining

values of 1.63 ± 0.13 for C5, 1.88 ± 0.08 for C9Z81 and 1.78 ± 0.08 for C13Z34 (Fig. 7b).

4. Discussion

Our results show by first time the identification of a new class of GRK2 inhibitors directed to the RH-Gαq PPIs with the capacity to induce a significant inhibition of receptor desensitization mediated by RH domain of GRK2.

GRK2 has been extensively validated as a pharmacological target for heart failure and hypertension treatment, and has been proposed as a promising one for other medical conditions such as Alzheimer's and Parkinson's diseases or even insulin resistance and diabetes [43–45]. Based on that, identification of small molecules that inhibit GRK2 actions is of great interest to confirm the role that this protein play in whole body physiology and for therapeutic purpose.

Many attempts have been done in order to identify promising GRK2 inhibitors. However, clinically useful small molecule inhibitors of GRK2 have yet to be described. The natural product balanol exhibits 50- and 100-fold selectivity for GRK2 over other members of the family; Takeda Pharmaceuticals Inc. 101 (CMPD101) and 103A exhibit similar potency of inhibition against GRK2 as that of balanol, but they have better selectivity for GRK2 over other GRKs and AGC kinases ($IC_{50} > 2 \mu M$) [46]. The selective serotonin reuptake inhibitor paroxetine has recently been shown to directly interact with the orthosteric site of GRK2 and to inhibit receptor desensitization by blocking GRK2-mediated adrenoceptor phosphorylation and arrestin recruitment [47] but is a much less potent inhibitor than balanol or the Takeda compounds. Based on that it seems like specific inhibition of GRK2 kinase activity is more striking than it looks like. Although many AGC kinases contain

additional regulatory domains or subunits, their catalytic cores are highly conserved making very difficult to obtain selective inhibitors [48].

On the other hand, phosphorylation of GPCRs by GRK2 and subsequent arrestin recruitment has been associated to protective signaling in the heart. Moreover, GRK2 kinase activity display an inhibitory function over cell proliferation and tumoral growth in several models [49]. Based on these observations alternative strategies to regulate GRK2 functions are of interest. Moreover, phosphorylation of GPCRs is not the only mechanism by which GRK2 may regulate GPCRs signaling. Expression of dominant negative mutants of RH domain has been shown to produce dramatic phenotypes. The expression of a GRK2-D110A mutant devoid in Gαq/11 binding increases mGluR5 signaling in response to agonist stimulation in striatal neurons [13]. GRK2-D110A partially reversed the quenching effect of GRK2, over inositol phosphate generation after histamine type 1 receptor stimulation [14]. GRK2 up-regulates the basal activity of the epithelial Na⁺ channel as a consequence of the binding of its RH domain the α-subunits of Gαq/11 [50]. In the same way, the RH domain of GRK2 proved to be involved in regulation of M1 and M3 mAChR [51,52]; mGluR1a glutamate receptor [53]; endothelin-1 A receptor [54] and histamine type 2 receptor [15]. These results suggest that a small molecule RH inhibitor might provide profound effects over GPCRs signaling.

We carried out a computer-aided drug design to discover new ligands based on GRK2 crystal structures. Inhibiting PPIs, such as the one between any member of RGS family of proteins and Gα subunits is particularly challenging, predominantly due to the size and geometry of the interaction interface that covers 750–1500 Å² [55] and the lack of well-defined traditional pockets [56]. However, DBVS directed to the biological relevant residues identified in the PPI surface between the RH domain

of GRK2 and the Gαq protein, allowed us the identification of candidates' inhibitors of the RH domain. PPI surface between other members of the RGS family of proteins and Gαq was identify as a druggable target in assays for bladder capacity and spontaneous bladder muscle contraction. In this system small molecules, BMS-192364 and BMS-195270, effectively affected the RGS/Gαq complex showing that small molecules affecting pathways downstream of GPCR function could represent potential new therapies for diseases characterized by inappropriate activation of GPCR signaling [57].

Our *in silico* screening allowed the reduction of the enormous chemical space to a manageable number of hits with the potentiality of binding to the RH domain of GRK2 and thus leading to a drug candidate. Molecules disrupting the interaction between the RH domain of GRK2 and Gαq should increase the magnitude and/or duration of G-protein signaling responses, leading to pronounced physiological effects. Therefore, the ability of candidates to inhibit GRK2 action was assessed as an increase in the calcium response of a GRK2 desensitized GPCR, the H1R, and as a diminished H1R desensitization. The action of compounds over the RH domain of GRK2 was confirmed using a dominant negative mutant of the RH domain of GRK2 (GRK2-D110A) where active compounds lost their effect. *In vitro* screening of candidates in a cellular context presented the advantage of determining a functional biological consequence of GRK2 inhibition instead of a mere interaction of compounds with the target which sometimes may not occur or fail in a conserved cellular context. However, since we only measured compounds effect over H1R regulation and GRK2 translocation we cannot rule out the possibility of interaction of compounds with other targets that may affect other pathways not evaluated in the present work.

Based on the chemical structure of the active compounds and the docking poses, it is likely that candidates present simple cyclic systems and amide groups. Interestingly, oxygen from amide group in C13Z34 is oriented towards Gln133 at an optimal distance to act as a hydrogen bond acceptor of NH from Gln133. Concerning that, crystallography of bovine GRK2 in interaction with Gαq shown that hydrogen bonds are formed between the side chains of Gαq-Thr260 and GRK2-Gln133 [40].

The RH domain of GRK2 has been shown to lack significant GTPase activity (GAP). Based on that, acceleration of GTP hydrolysis may not be its mechanism of action [58,59]. However, it has been described that the RGS family of proteins may also regulate signaling by occlusion on Gα of the binding site for effector in a mechanism known as effector antagonism [60]. It has been described that the GRK2 RH domain binds Gαq more like an effector than an RGS protein [40,59]. In this direction, results obtained showed that our inhibitors blocked both Gαq-coupled receptor desensitization and constitutively active Gαq mediated translocation of GRK2, indicating that GRK2 may bind to and sequester Gαq subunit reducing the pool of receptor-regulated G proteins and hence, the effects of agonists leading to receptor desensitization. Such mechanism has been described for other members of RGS family of proteins regarding μ-opioid and muscarinic M3 receptors desensitization in the central nervous system [61, 62]. Interestingly, C13Z34 also affected a phosphorylation dependent mechanism as H1R internalization. However, since C13Z34 proved to block GRK2 translocation to plasma membrane, this blockage may be the cause of the attenuation of internalization rather than an inhibition of kinase activity by C13Z34 [31, 63, 64].

Finally, we preliminary studied preclinical pharmacology of candidates to obtain useful information for their future use and optimization. Toxicity issues are an

important cause of drug failure in the clinic. Safety assessment of compounds through cytotoxicity assays suggests that our candidates are safe at effective concentrations. In the other hand, lipophilicity is a key physicochemical property of drugs that impacts not only in their pharmacokinetics, but also in their pharmacodynamic and toxicological profile. LogK_w values obtained for our compounds are within the optimum region of lipophilicity that comprises values from 1 to 3, contributing to their quality as candidate drugs [65].

Our strategy was successful at identifying new compounds that not only showed high potency against GRK2 mediated desensitization, but also presented adequate ADMET properties. This evidence supports the DBVS approach proposed in this work and sets the basis to continue investigating the mechanism of action of these candidates through the inhibition of the RH domain of GRK2.

5. Conclusions

By docking-based virtual screening we identified inhibitors of the RH domain of GRK2.

Active compounds were able to increase H1R response and reduce the RH mediated desensitization of the H1R.

Inhibitors also blocked GRK2 translocation to plasma membrane and diminished GRK2 mediated internalization of H1R.

Active compounds presented adequate ADMET properties.

Competing interests´ statement

None.

Acknowledgments:

This work was supported by grants from: Universidad de Buenos Aires (UBACyT 20020130100624BA); Agencia Nacional de Promoción Científica y Tecnológica (PICT 2013 N°2050, PICT 2015 N° 2443); and Consejo Nacional de Investigaciones Científicas y Técnicas (2013-2015 PIP 562).

Bibliography

- [1] Sriram K, Insel PA. G Protein-Coupled Receptors as Targets for Approved Drugs: How Many Targets and How Many Drugs? *Mol Pharmacol* 2018;93:251–8. doi:10.1124/mol.117.111062.
- [2] Ribas C, Penela P, Murga C, Salcedo A, García-Hoz C, Jurado-Pueyo M, et al. The G protein-coupled receptor kinase (GRK) interactome: role of GRKs in GPCR regulation and signaling. *Biochim Biophys Acta* 2007;1768:913–22. doi:10.1016/j.bbame.2006.09.019.
- [3] Mushegian A, Gurevich VV, Gurevich EV. The origin and evolution of G protein-coupled receptor kinases. *PLoS ONE* 2012;7:e33806. doi:10.1371/journal.pone.0033806.
- [4] Watari K, Nakaya M, Kurose H. Multiple functions of G protein-coupled receptor kinases. *J Mol Signal* 2014;9:1. doi:10.1186/1750-2187-9-1.
- [5] Penela P, Ribas C, Mayor F. Mechanisms of regulation of the expression and function of G protein-coupled receptor kinases. *Cell Signal* 2003;15:973–81. doi:10.1016/S0898-6568(03)00099-8.
- [6] Benovic JL, DeBlasi A, Stone WC, Caron MG, Lefkowitz RJ. Beta-adrenergic receptor kinase: primary structure delineates a multigene family. *Science*

- 1989;246:235–40. doi:10.1126/science.2552582.
- [7] Schumacher SM, Koch WJ. Noncanonical Roles of G Protein-coupled Receptor Kinases in Cardiovascular Signaling. *J Cardiovasc Pharmacol* 2017;70:129–41. doi:10.1097/FJC.0000000000000483.
- [8] Steury MD, McCabe LR, Parameswaran N. G Protein-Coupled Receptor Kinases in the Inflammatory Response and Signaling. *Adv Immunol* 2017;136:227–77. doi:10.1016/bs.ai.2017.05.003.
- [9] Obrenovich ME, Palacios HH, Gasimov E, Leszek J, Aliev G. The GRK2 Overexpression Is a Primary Hallmark of Mitochondrial Lesions during Early Alzheimer Disease. *Cardiovasc Psychiatry Neurol* 2009;2009:327360. doi:10.1155/2009/327360.
- [10] Murga C, Arcones AC, Cruces-Sande M, Briones AM, Salaices M, Mayor F. G Protein-Coupled Receptor Kinase 2 (GRK2) as a Potential Therapeutic Target in Cardiovascular and Metabolic Diseases. *Front Pharmacol* 2019;10:112. doi:10.3389/fphar.2019.00112.
- [11] Han C, Li Y, Wang Y, Cui D, Luo T, Zhang Y, et al. Development of Inflammatory Immune Response-Related Drugs Based on G Protein-Coupled Receptor Kinase 2. *Cell Physiol Biochem* 2018;51:729–45. doi:10.1159/000495329.
- [12] Raveh A, Cooper A, Guy-David L, Reuveny E. Nonenzymatic rapid control of GIRK channel function by a G protein-coupled receptor kinase. *Cell* 2010;143:750–60. doi:10.1016/j.cell.2010.10.018.
- [13] Ribeiro FM, Ferreira LT, Paquet M, Cregan T, Ding Q, Gros R, et al. Phosphorylation-independent regulation of metabotropic glutamate receptor 5 desensitization and internalization by G protein-coupled receptor kinase 2 in

- neurons. *J Biol Chem* 2009;284:23444–53. doi:10.1074/jbc.M109.000778.
- [14] Iwata K, Luo J, Penn RB, Benovic JL. Bimodal regulation of the human H1 histamine receptor by G protein-coupled receptor kinase 2. *J Biol Chem* 2005;280:2197–204. doi:10.1074/jbc.M408834200.
- [15] Fernandez N, Gottardo FL, Alonso MN, Monczor F, Shayo C, Davio C. Roles of phosphorylation-dependent and -independent mechanisms in the regulation of histamine H2 receptor by G protein-coupled receptor kinase 2. *J Biol Chem* 2011;286:28697–706. doi:10.1074/jbc.M111.269613.
- [16] Aziziyeh AI, Li TT, Pape C, Pampillo M, Chidiac P, Possmayer F, et al. Dual regulation of lysophosphatidic acid (LPA1) receptor signalling by Ral and GRK. *Cell Signal* 2009;21:1207–17. doi:10.1016/j.cellsig.2009.03.011.
- [17] Reiter E, Marion S, Robert F, Troispoux C, Boulay F, Guillou F, et al. Kinase-inactive G-protein-coupled receptor kinases are able to attenuate follicle-stimulating hormone-induced signaling. *Biochem Biophys Res Commun* 2001;282:71–8. doi:10.1006/bbrc.2001.4534.
- [18] Namkung Y, Dipace C, Urizar E, Javitch JA, Sibley DR. G protein-coupled receptor kinase-2 constitutively regulates D2 dopamine receptor expression and signaling independently of receptor phosphorylation. *J Biol Chem* 2009;284:34103–15. doi:10.1074/jbc.M109.055707.
- [19] Evron T, Daigle TL, Caron MG. GRK2: multiple roles beyond G protein-coupled receptor desensitization. *Trends Pharmacol Sci* 2012;33:154–64. doi:10.1016/j.tips.2011.12.003.
- [20] Sallese M, Mariggiò S, D'Urbano E, Iacovelli L, De Blasi A. Selective regulation of Gq signaling by G protein-coupled receptor kinase 2: direct interaction of kinase N terminus with activated galphaq. *Mol Pharmacol*

- 2000;57:826–31.
- [21] Usui H, Nishiyama M, Moroi K, Shibasaki T, Zhou J, Ishida J, et al. RGS domain in the amino-terminus of G protein-coupled receptor kinase 2 inhibits Gq-mediated signaling. *Int J Mol Med* 2000. doi:10.3892/ijmm.5.4.335.
- [22] Han C-C, Ma Y, Li Y, Wang Y, Wei W. Regulatory effects of GRK2 on GPCRs and non-GPCRs and possible use as a drug target (Review). *Int J Mol Med* 2016;38:987–94. doi:10.3892/ijmm.2016.2720.
- [23] Sorriento D, Ciccarelli M, Cipolletta E, Trimarco B, Iaccarino G. “Freeze, Don’t Move”: How to Arrest a Suspect in Heart Failure - A Review on Available GRK2 Inhibitors. *Front Cardiovasc Med* 2016;3:48. doi:10.3389/fcvm.2016.00048.
- [24] Homan KT, Tesmer JJG. Molecular basis for small molecule inhibition of G protein-coupled receptor kinases. *ACS Chem Biol* 2015;10:246–56. doi:10.1021/cb5003976.
- [25] Monzon AM, Rohr CO, Fornasari MS, Parisi G. CoDNaS 2.0: a comprehensive database of protein conformational diversity in the native state. *Database (Oxford)* 2016;2016. doi:10.1093/database/baw038.
- [26] Schmidtke P, Le Guilloux V, Maupetit J, Tufféry P. fpocket: online tools for protein ensemble pocket detection and tracking. *Nucleic Acids Res* 2010;38:W582-9. doi:10.1093/nar/gkq383.
- [27] Hubbard S, Thornton J (1993) NACCESS. Computer Program, Department of Biochemistry and Molecular Biology, University College London. - Open Access Library n.d. <http://www.oalib.com/references/5299711> (accessed April 15, 2019).
- [28] Trott O, Olson AJ. AutoDock Vina: improving the speed and accuracy of

- docking with a new scoring function, efficient optimization, and multithreading. J Comput Chem 2010;31:455–61. doi:10.1002/jcc.21334.
- [29] Morris GM, Huey R, Olson AJ. Using AutoDock for ligand-receptor docking. Curr Protoc Bioinformatics 2008;Chapter 8:Unit 8.14. doi:10.1002/0471250953.bi0814s24.
- [30] Glisoni RJ, Chiappetta DA, Finkielstein LM, Moglioni AG, Sosnik A. Self-aggregation behaviour of novel thiosemicarbazone drug candidates with potential antiviral activity. New J Chem 2010;34:2047. doi:10.1039/c0nj00061b.
- [31] Sterne-Marr R, Dhimi GK, Tesmer JJG, Ferguson SSG. Characterization of GRK2 RH domain-dependent regulation of GPCR coupling to heterotrimeric G proteins. Meth Enzymol 2004;390:310–36. doi:10.1016/S0076-6879(04)90020-1.
- [32] Hasenahuer MA, Barletta GP, Fernandez-Alberti S, Parisi G, Fornasari MS. Correction: Pockets as structural descriptors of EGFR kinase conformations. PLoS ONE 2018;13:e0192815. doi:10.1371/journal.pone.0192815.
- [33] Bogan AA, Thorn KS. Anatomy of hot spots in protein interfaces. J Mol Biol 1998;280:1–9. doi:10.1006/jmbi.1998.1843.
- [34] Zoete V, Michielin O, Karplus M. Relation between sequence and structure of HIV-1 protease inhibitor complexes: a model system for the analysis of protein flexibility. J Mol Biol 2002;315:21–52. doi:10.1006/jmbi.2001.5173.
- [35] Koshland DE. Conformational changes: how small is big enough? Nat Med 1998;4:1112–4. doi:10.1038/2605.
- [36] Buonfiglio R, Recanatini M, Masetti M. Protein flexibility in drug discovery: from theory to computation. ChemMedChem 2015;10:1141–8.

- doi:10.1002/cmdc.201500086.
- [37] Touw WG, Baakman C, Black J, te Beek TAH, Krieger E, Joosten RP, et al. A series of PDB-related databanks for everyday needs. *Nucleic Acids Res* 2015;43:D364-8. doi:10.1093/nar/gku1028.
- [38] Sterne-Marr R, Tesmer JJG, Day PW, Stracquatano RP, Cilente J-AE, O'Connor KE, et al. G protein-coupled receptor Kinase 2/G alpha q/11 interaction. A novel surface on a regulator of G protein signaling homology domain for binding G alpha subunits. *J Biol Chem* 2003;278:6050–8. doi:10.1074/jbc.M208787200.
- [39] Darnell SJ, LeGault L, Mitchell JC. KFC Server: interactive forecasting of protein interaction hot spots. *Nucleic Acids Res* 2008;36:W265-9. doi:10.1093/nar/gkn346.
- [40] Tesmer VM, Kawano T, Shankaranarayanan A, Kozasa T, Tesmer JJG. Snapshot of activated G proteins at the membrane: the Galphaq-GRK2-Gbetagamma complex. *Science* 2005;310:1686–90. doi:10.1126/science.1118890.
- [41] Tesmer JJG, Tesmer VM, Lodowski DT, Steinhagen H, Huber J. Structure of human G protein-coupled receptor kinase 2 in complex with the kinase inhibitor balanol. *J Med Chem* 2010;53:1867–70. doi:10.1021/jm9017515.
- [42] Day PW, Wedegaertner PB, Benovic JL. Analysis of G-protein-coupled receptor kinase RGS homology domains. *Meth Enzymol* 2004;390:295–310. doi:10.1016/S0076-6879(04)90019-5.
- [43] Cipolletta E, Gambardella J, Fiordelisi A, Del Giudice C, Di Vaia E, Ciccarelli M, et al. Antidiabetic and Cardioprotective Effects of Pharmacological Inhibition of GRK2 in db/db Mice. *Int J Mol Sci* 2019;20. doi:10.3390/ijms20061492.

- [44] Sakamoto M, Arawaka S, Hara S, Sato H, Cui C, Machiya Y, et al. Contribution of endogenous G-protein-coupled receptor kinases to Ser129 phosphorylation of alpha-synuclein in HEK293 cells. *Biochem Biophys Res Commun* 2009;384:378–82. doi:10.1016/j.bbrc.2009.04.130.
- [45] Obrenovich ME, Morales LA, Cobb CJ, Shenk JC, Méndez GM, Fischbach K, et al. Insights into cerebrovascular complications and Alzheimer disease through the selective loss of GRK2 regulation. *J Cell Mol Med* 2009;13:853–65. doi:10.1111/j.1582-4934.2008.00512.x.
- [46] Okawa T, Aramaki Y, Yamamoto M, Kobayashi T, Fukumoto S, Toyoda Y, Henta T, Hata A, Ikeda S, Kaneko M, Hoffman ID, Sang BC, Zou H, Kawamoto T. Design, Synthesis, and Evaluation of the Highly Selective and Potent G-Protein-Coupled Receptor Kinase 2 (GRK2) Inhibitor for the Potential Treatment of Heart Failure. *J Med Chem*. 2017 Aug 24;60(16):6942-6990. doi: 10.1021/acs.jmedchem.7b00443.
- [47] Guo S, Carter RL, Grisanti LA, Koch WJ, Tilley DG. Impact of paroxetine on proximal β -adrenergic receptor signaling. *Cell Signal* 2017;38:127–33. doi:10.1016/j.cellsig.2017.07.006.
- [48] Leroux AE, Schulze JO, Biondi RM. AGC kinases, mechanisms of regulation and innovative drug development. *Semin Cancer Biol* 2018;48:1–17. doi:10.1016/j.semcancer.2017.05.011.
- [49] Fu X, Koller S, Abd Alla J, Quitterer U. Inhibition of G-protein-coupled receptor kinase 2 (GRK2) triggers the growth-promoting mitogen-activated protein kinase (MAPK) pathway. *J Biol Chem* 2013;288:7738–55. doi:10.1074/jbc.M112.428078.
- [50] Lee I-H, Song S-H, Campbell CR, Kumar S, Cook DI, Dinudom A. Regulation

- of the epithelial Na⁺ channel by the RH domain of G protein-coupled receptor kinase, GRK2, and Galphaq/11. *J Biol Chem* 2011;286:19259–69. doi:10.1074/jbc.M111.239772.
- [51] Willets JM, Nahorski SR, Challiss RAJ. Roles of phosphorylation-dependent and -independent mechanisms in the regulation of M1 muscarinic acetylcholine receptors by G protein-coupled receptor kinase 2 in hippocampal neurons. *J Biol Chem* 2005;280:18950–8. doi:10.1074/jbc.M412682200.
- [52] Luo J, Busillo JM, Benovic JL. M3 muscarinic acetylcholine receptor-mediated signaling is regulated by distinct mechanisms. *Mol Pharmacol* 2008;74:338–47. doi:10.1124/mol.107.044750.
- [53] Dhami GK, Dale LB, Anborgh PH, O'Connor-Halligan KE, Sterne-Marr R, Ferguson SSG. G Protein-coupled receptor kinase 2 regulator of G protein signaling homology domain binds to both metabotropic glutamate receptor 1a and Galphaq to attenuate signaling. *J Biol Chem* 2004;279:16614–20. doi:10.1074/jbc.M314090200.
- [54] Gärtner F, Seidel T, Schulz U, Gummert J, Milting H. Desensitization and internalization of endothelin receptor A: impact of G protein-coupled receptor kinase 2 (GRK2)-mediated phosphorylation. *J Biol Chem* 2013;288:32138–48. doi:10.1074/jbc.M113.461566.
- [55] Arkin MR, Wells JA. Small-molecule inhibitors of protein-protein interactions: progressing towards the dream. *Nat Rev Drug Discov* 2004;3:301–17. doi:10.1038/nrd1343.
- [56] Blazer LL, Neubig RR. Small molecule protein-protein interaction inhibitors as CNS therapeutic agents: current progress and future hurdles. *Neuropsychopharmacology* 2009;34:126–41. doi:10.1038/npp.2008.151.

- [57] Storaska AJ, Mei JP, Wu M, Li M, Wade SM, Blazer LL, et al. Reversible inhibitors of regulators of G-protein signaling identified in a high-throughput cell-based calcium signaling assay. *Cell Signal* 2013;25:2848–55. doi:10.1016/j.cellsig.2013.09.007.
- [58] Carman CV, Parent JL, Day PW, Pronin AN, Sternweis PM, Wedegaertner PB, et al. Selective regulation of G α (q/11) by an RGS domain in the G protein-coupled receptor kinase, GRK2. *J Biol Chem* 1999;274:34483–92.
- [59] Tesmer JJ, Berman DM, Gilman AG, Sprang SR. Structure of RGS4 bound to AIF4--activated G(i α 1): stabilization of the transition state for GTP hydrolysis. *Cell* 1997;89:251–61.
- [60] Hepler JR, Berman DM, Gilman AG, Kozasa T. RGS4 and GAIIP are GTPase-activating proteins for Gq α and block activation of phospholipase C β by gamma-thio-GTP-Gq α . *Proc Natl Acad Sci USA* 1997;94:428–32.
- [61] Anger T, Zhang W, Mende U. Differential contribution of GTPase activation and effector antagonism to the inhibitory effect of RGS proteins on Gq-mediated signaling in vivo. *J Biol Chem* 2004;279:3906–15. doi:10.1074/jbc.M309496200.
- [62] Garzón J, Rodríguez-Muñoz M, de la Torre-Madrid E, Sánchez-Blázquez P. Effector antagonism by the regulators of G protein signalling (RGS) proteins causes desensitization of mu-opioid receptors in the CNS. *Psychopharmacology (Berl)* 2005;180:1–11. doi:10.1007/s00213-005-2248-9.
- [63] Desai AN, Salim S, Standifer KM, Eikenburg DC. Involvement of G protein-coupled receptor kinase (GRK) 3 and GRK2 in down-regulation of the α 2B-adrenoceptor. *J Pharmacol Exp Ther*. 2006 Jun;317(3):1027-35.
- [64] Wolters V, Krasel C, Brockmann J, Bünemann M. Influence of G α q on the

dynamics of m3-acetylcholine receptor-g-protein-coupled receptor kinase 2 interaction. *Mol Pharmacol.* 2015 Jan;87(1):9-17. doi: 0.1124/mol.114.094722.

[65] Arnott JA, Planey SL. The influence of lipophilicity in drug discovery and design. *Expert Opin Drug Discov* 2012;7:863–75. doi:10.1517/17460441.2012.714363.

Figure Legends

Figure 1. Selection of specific molecular target in RH domain of GRK2. **a.** Z-score calculated by the C-alpha RMSD per position of the maximum-pair of conformers. Dotted lines indicate the R106 and Q133 residues. **b.** Crystal structure of bovine GRK2 (RH domain: red, kinase domain: blue, PH domain: yellow ribbons) in complex with $G\alpha_q$ subunit (Grey ribbons) corresponding to PDB ID 2BCJ. PPI interface between both proteins is indicated through surface representation. **c.** Residues predicted by the KFC Server to be energetically important for the PPI occurrence are shown in purple font. Residues that when mutated alter GRK2 binding to $G\alpha_q$ are in boxes. **d.** Final location of grid box used for DBVS in crystal structure of human GRK2 corresponding to pdb ID 3KRW.

Figure 2. C1-C15 compounds acquired from Enamine. Chemical structures, identifier code (Z) and docking score (S) of compounds are shown.

Figure 3. Validation of the cellular model used in biological activity screening of selected compounds. A549 cells were loaded with Fura-2AM dye, ($\lambda_{excitation}$ $Ca^{2+}_{saturated}$: 340nm, $\lambda_{excitation}$ Ca^{2+}_{free} : 380nm) and fluorescence (F) was measured in

real time experiments. At 180s Triton 1.6% was added as a control of effective dye incorporation into the cell. Intracellular Ca^{2+} levels were determined as F_{340}/F_{380} normalized respect to basal and maximum values. **a.** Response assays were performed in A549 cells loaded with Fura-2AM by stimulation with increasing concentrations of histamine (HA) at 30 s of measurement (left panel). Desensitization assays were performed in A549 cells loaded with Fura-2AM by pretreatment with increasing concentrations of HA during 10 min, and stimulation with 100 μM HA at 30 s of measurement (right panel). Data from a single experiment is shown and is representative of four independent experiments. (*) $P<0.05$, (**) $P<0.01$ (***) $P<0.005$ respect to base line (left panel) or control without treatment (right panel). **b.** A549 cells were transiently transfected with GRK2-D110A plasmid or empty vector (Mock) and loaded with Fura-2AM. Both were used to perform response and desensitization (with 100 μM HA) assays (left panel). Overexpression of GRK2 variant was verified by Western Blot (right panel). Data from a single experiment is shown and is representative of three independent experiments. (*) $P<0.05$, (**) $P<0.005$, (ns) no significant differences, respect to Mock control without pretreatment. Comparisons were made using Two-way ANOVA followed by the Tukey's post-test.

Figure 4. Biological activity of hit compounds: Specific positive modulation of calcium response. A549 cells were loaded with Fura-2AM dye, ($\lambda_{\text{excitation}}$ Ca^{2+} -saturated: 340nm, $\lambda_{\text{excitation}}$ Ca^{2+} -free: 380nm) and fluorescence (F) was measured in real time experiments. At 180 s Triton 1.6% was added as a control of effective dye incorporation into the cell. Intracellular Ca^{2+} levels were determined as F_{340}/F_{380} normalized respect to basal and maximum values. **a.** A549 cells loaded with Fura-

2AM were pretreated with 100nM of C1-C15 or DMSO for 40 min, and response and desensitization assays were performed. Results for all positive compounds C5Z29, C9Z81 and C13Z34; and one example of a negative compound C7Z64 are shown. Comparisons were made using Two-way ANOVA followed by the Tukey's post-test. Different letters indicate statistically significant differences. (***) $P < 0.005$ respect to control without treatment; (###) respect to desensitized cells in presence of vehicle DMSO; (ns) no significant differences respect to vehicle DMSO for control or desensitized cells **b**. A549 cells were transiently transfected with GRK2 D110A plasmid, loaded with Fura-2AM and used to perform response and desensitization (with 100 μ M HA) assays. **c**. Direct effect of compounds over intracellular calcium levels was evaluated by stimulation of Fura-2AM loaded A549 cells with 100nM of compound or DMSO at 30 s of measurement. Data from a single experiment is shown and is representative of three independent experiments.

Figure 5. Biological activity of C13Z34. A549 cells were loaded with Fura-2AM dye, ($\lambda_{\text{excitation Ca}^{2+}\text{-saturated}}$: 340nm, $\lambda_{\text{excitation Ca}^{2+}\text{-free}}$: 380nm) and fluorescence (F) was measured in real time experiments. At 180 s Triton 1.6% was added as a control of effective dye incorporation into the cell. Intracellular Ca^{2+} levels were determined as F_{340}/F_{380} normalized respect to basal and maximum values. **a**. A549 cells loaded with Fura-2AM were pretreated with increasing concentrations of C13 for 40 min, and desensitization assays were performed (left panel). The maximum Ca^{++} response obtained for each C13Z34 concentration was used to build a concentration-response curve (right panel). Data from a single experiment is shown and is representative of three independent experiments. **b**. A549 cells were transiently transfected with GRK2 K220R plasmid or empty vector (Mock), loaded

with Fura-2AM and pretreated with 100nM of C13Z34 or DMSO. Both were used to perform desensitization (with 100 μ M HA) assays (left panel) (*) $P < 0.05$, (ns) no significant differences, respect to vehicle DMSO in Mock transfected cells. Overexpression of GRK2 variant was verified by Western Blot (right panel). Data from a single experiment is shown and is representative of three independent experiments. Comparisons were made using Two-way ANOVA followed by the Tukey's post-test. Different letters indicate statistically significant differences. The level of significance was set at $P < 0.05$. **c.** A549 cells loaded with Fura-2AM were pretreated with 10 μ M of CMPD101 or DMSO for 40 min, and response and desensitization assays were performed. Data from a single experiment is shown, and is representative of three independent experiments. **d.** A549 cells were pretreated with 100nM of C13Z34 or 10 μ M of CMPD101 for 80 min and with HA 100 μ M for the last 60 minutes, washed and incubated with different concentrations of [3 H]mepyramine as stated in Materials and Methods. Data represent media \pm SEM of three independent experiments. **e.** Ligand binding pockets for the most energetically favorable conformation of C13Z34 in GRK2. Druggable pocket identified by F_{pocket} is colored in blue and biologically relevant residues (Arg106 and Gln133) are colored in green (left panel). Residues of RGS in close contacts 34 are shown (right panels).

Figure 6. Biological activity of hit compounds: Inhibition of GRK2(45-178)GFP translocation. **a.** HeLa cells were transiently cotransfected with GRK2(45-178)GFP plasmid and G α qQL (constitutively active) or empty vector, and fixed after 48hs. Subcellular localization was assessed by confocal microscopy. **b.** HeLa cells were transiently cotransfected with GRK2(45-178)GFP plasmid and G α qQL. 48hs after

transfection cells were treated with 100nM of C5Z29, C9Z81, C13Z34, C7Z64 (negative control) or DMSO (vehicle control) during 40min and fixed.

At least 100 cells were examined in three independent experiments. For each cell in a given image, a line intensity profile across the cell was obtained. Representative intensity profiles are shown in yellow for each condition.

Figure 7. Preliminary profiling of physicochemical and in vitro ADMET properties of hit compounds. **a.** HepG2 (left panel) and U937 (right panel) cells were treated with increasing concentrations of C5Z29, C9Z81, C13Z34 or DMSO during 48hs, and cell viability was determined by Trypan Blue exclusion test. Data represent media \pm SD of three independent experiments **b.** Lipophilicity of hit compounds was determined by RP-HPLC as detailed in Methods section. Processing of retention time “RT” and dead time “T₀” (solvent front, DMSO) for each compound is shown. Experimental log K_w values correspond to extrapolations at 0% acetonitrile (ACN).

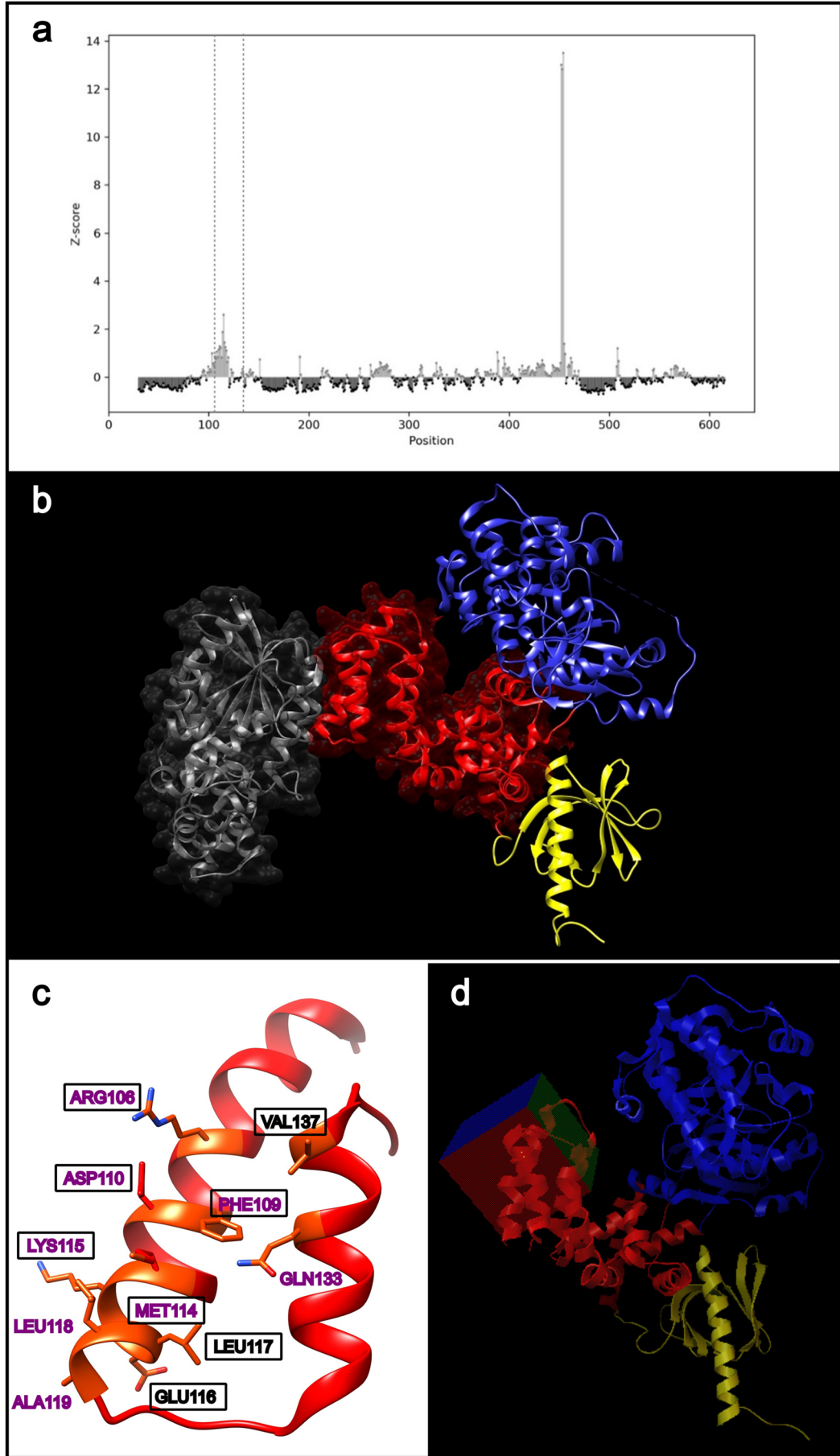


Figure 1

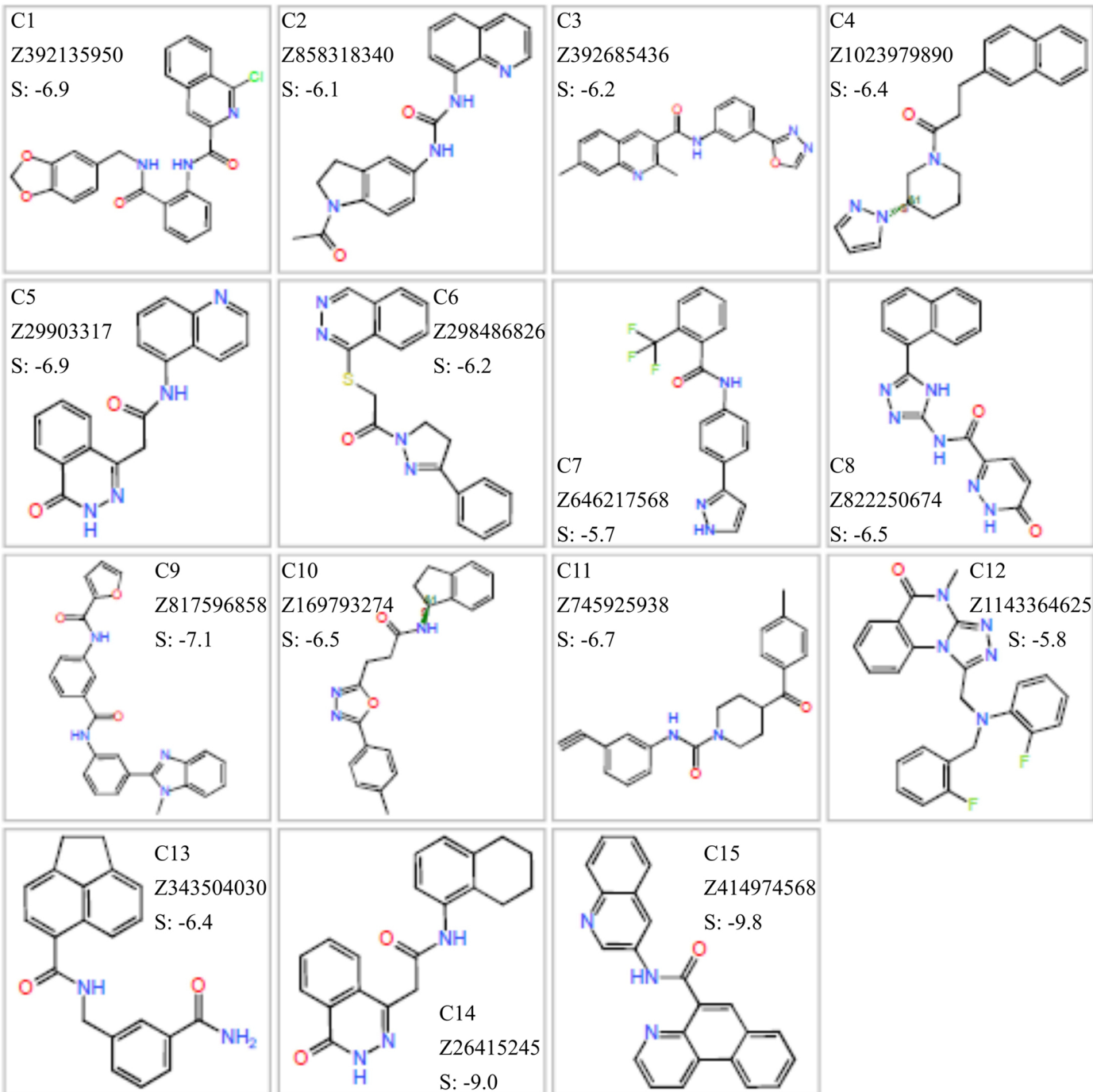
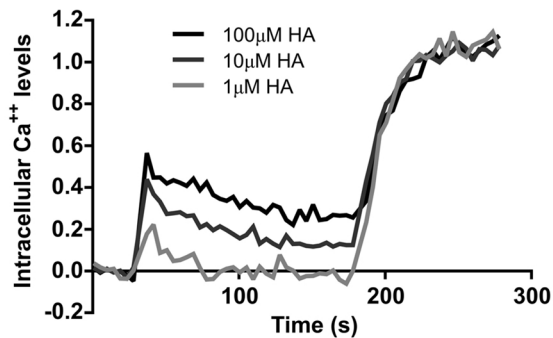
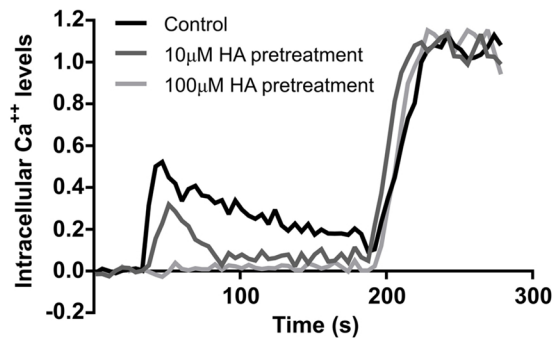


Figure 2

a

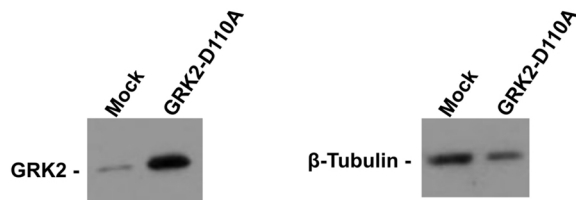
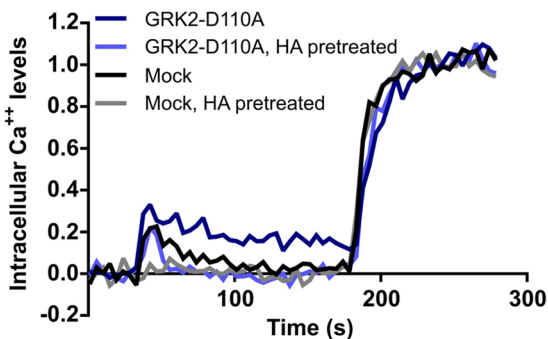


Condition	Maximum Ca ²⁺ response
1µM Histamine	0.199±0.066 (*)
10µM Histamine	0.419±0.067 (**)
100µM Histamine	0.565±0.058 (***)



Condition	Maximum Ca ²⁺ response
Control	0.513±0.166
10µM HA pretreatment	0.301±0.057 (**)
100µM HA pretreatment	0.024±0.025 (***)

b



Condition	Maximum Ca ²⁺ response
Mock	0.218±0.045
Mock, HA pretreated	0.044±0.043 (***)
GRK2-D110A	0.330±0.044 (*)
GRK2-D110A, HA pretreated	0.224±0.038 (ns)

Figure 3

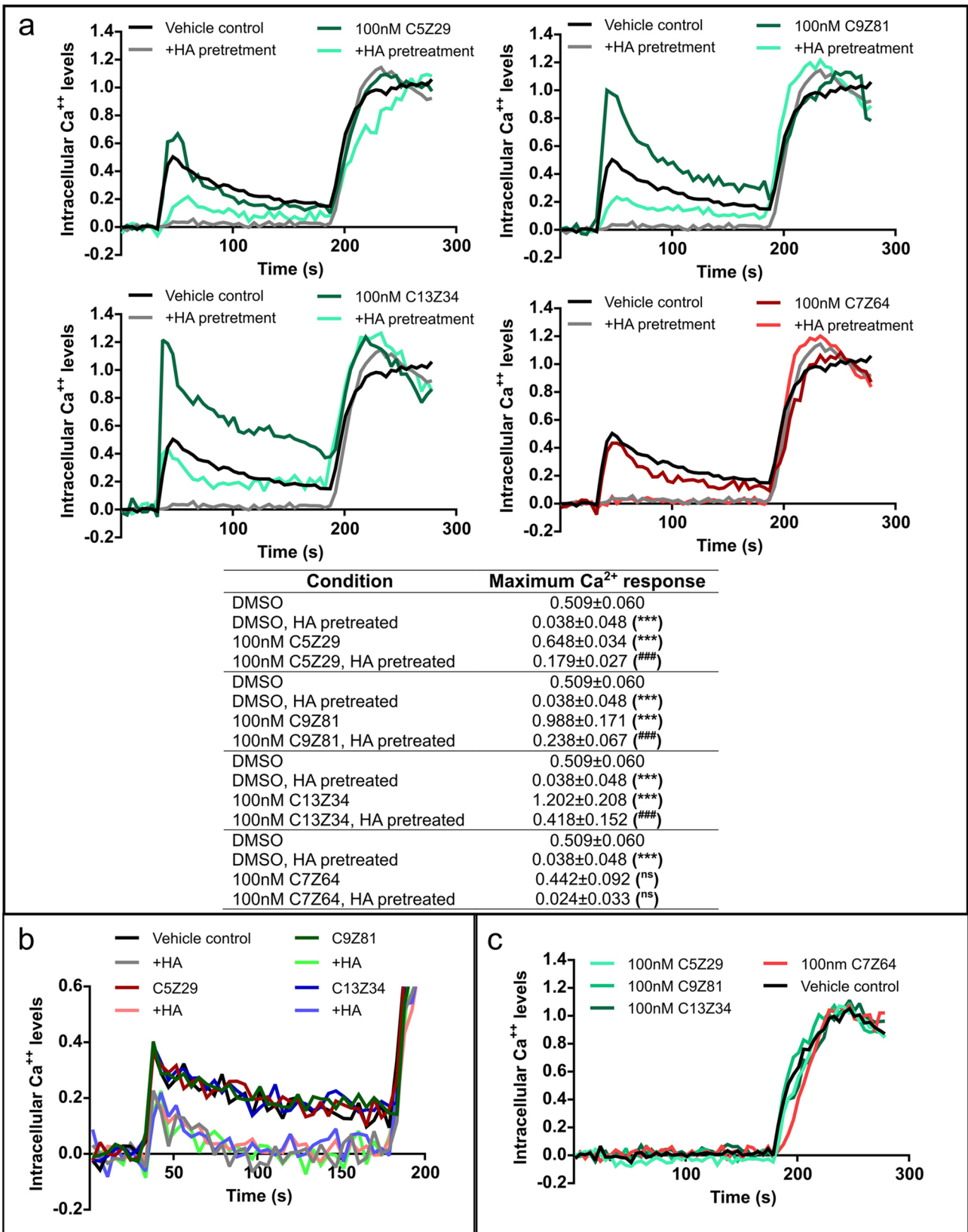


Figure 4

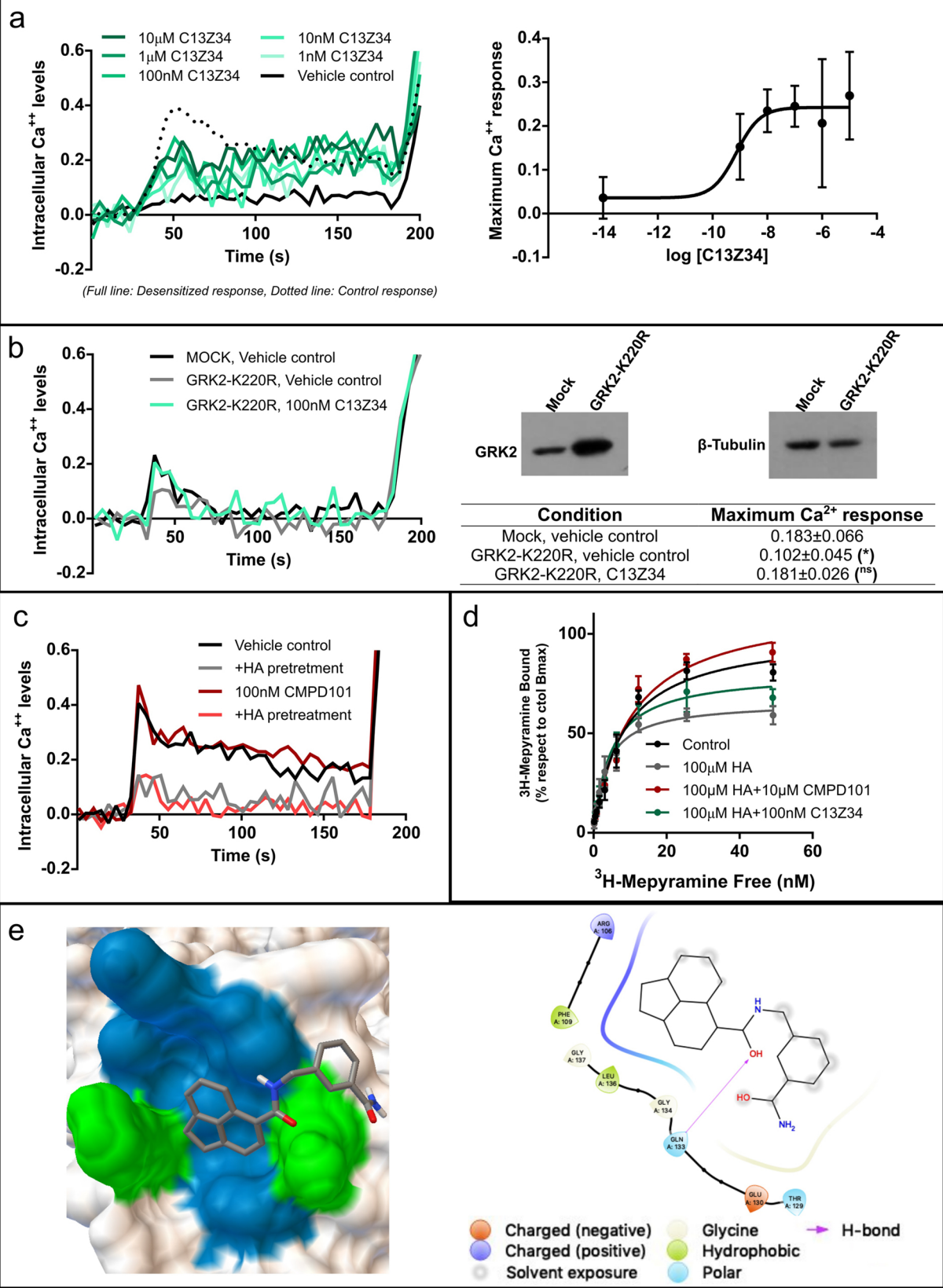


Figure 5

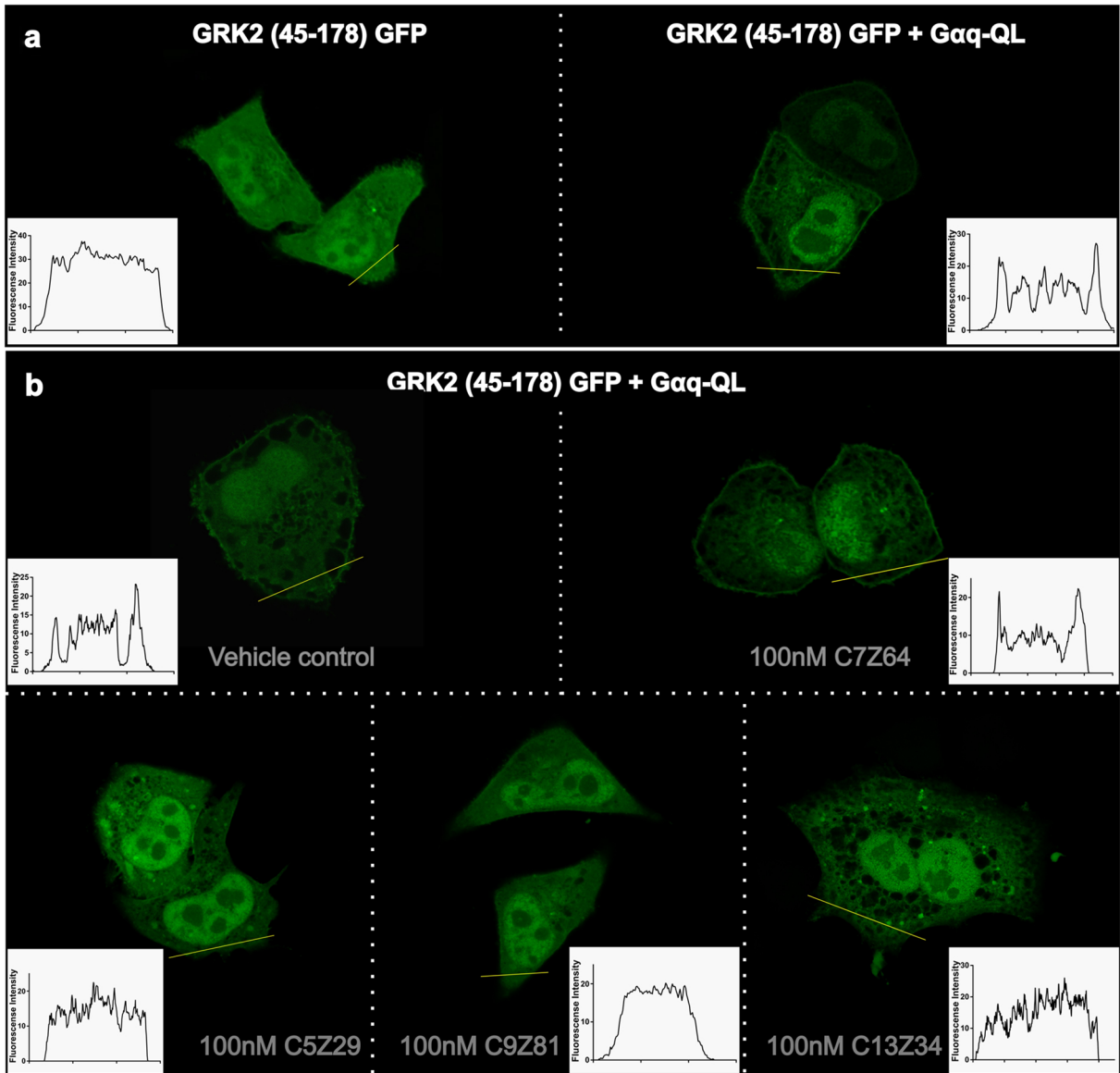


Figure 6

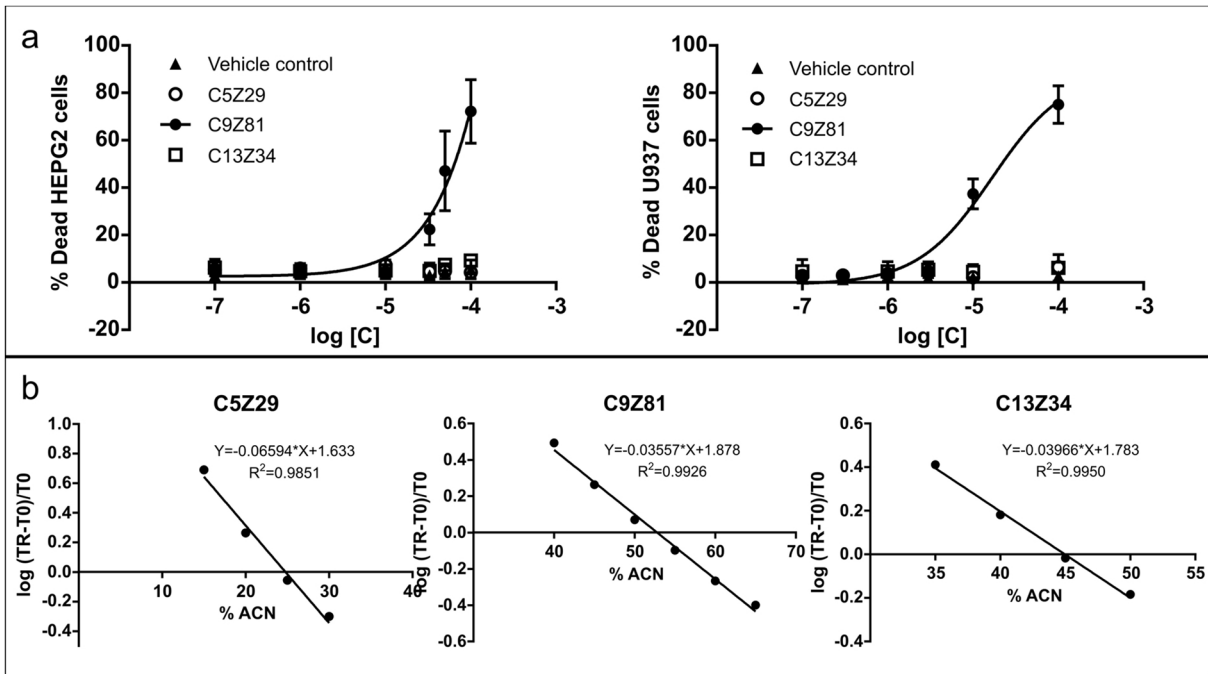


Figure 7